Unintegrated parton distributions

M.A. Kimber[a], A.D. Martin[a] and M.G. Ryskin[a,b]

[a] Department of Physics, University of Durham, Durham, DH1 3LE
[b] Petersburg Nuclear Physics Institute, Gatchina, St. Petersburg, 188300, Russia

Abstract

We describe how to calculate the parton distributions $f_a(x, k_t^2, \mu^2)$, unintegrated over the parton transverse momentum k_t, from auxiliary functions $h_a(x, k_t^2)$, which satisfy single-scale evolution equations. The formalism embodies both DGLAP and BFKL contributions, and accounts for the angular ordering which comes from coherence effects in gluon emission. We check that the unintegrated distributions give the measured values of the deep inelastic structure function $F_2(x, Q^2)$.

1 Introduction

Conventionally deep inelastic lepton-proton scattering is described in terms of scale-dependent parton distributions, $a(x, \mu^2)$, where $a = xg$ or xq. These distributions correspond to the density of partons in the proton with longitudinal momentum fraction x, integrated over transverse momentum up to $k_t = \mu$. They satisfy DGLAP evolution in μ^2. The kinematic region $k_t < \mu$ gives the leading $\ln \mu^2$ approximation to deep inelastic scattering.

For less inclusive processes it is, however, necessary to consider distributions unintegrated over the transverse momentum k_t of the parton. The unintegrated distributions have the advantage that they exactly correspond to the quantity which enters the Feynman diagrams and therefore allow for the true kinematics of the process even at leading order (LO). These

arXiv:hep-ph/0101348v1 31 Jan 2001

distributions $f_a(x, k_t^2, \mu^2)$ depend on two hard scales[1]: k_t and the scale μ of the probe. The scale μ plays a dual role. On the one hand it acts as the factorization scale, while on the other hand it controls the angular ordering of the partons emitted in the evolution [1].

Clearly it is desirable to also include $\ln(1/x)$ BFKL-type contributions in the evolution. Recall that both DGLAP and BFKL evolution are essentially equivalent to ordered evolution in the angles of the emitted partons[2]. In the DGLAP collinear approximation the angle increases due to the growth of k_t, while in BFKL the angle ($\theta \simeq k_t/k_\ell$) grows due to the decreasing longitudinal momentum fraction as we proceed along the emission chain from the proton. The factorization scale μ separates the partons associated with emission from different parts of the process, that is from the beam and target protons (in pp collisions) and from the hard subprocess. For example it separates emissions from the beam (with polar angle $\theta \lesssim 90°$) from those from the target (with $\theta \gtrsim 90°$), and from the intermediate partons from the hard subprocess. This separation was proved in Ref. [1] and originates from the destructive interference of the different emission amplitudes in the angular boundary regions. If the longitudinal momentum fraction is fixed by the hard subprocess, then the limits on the angles can be expressed in terms of a factorization scale μ which corresponds to the upper limit[3] on the allowed values of the (s-channel) parton k_t.

Since the parton distributions depend on two scales we potentially have to deal with complicated (CCFM [1]) evolution equations for the $f_a(x, k_t^2, \mu^2)$ functions. Of course it is possible to work with two-scale distributions, but this is much more complicated [2] and up to now has only proved practical with Monte Carlo generators [3]. However, the evolution process is essentially controlled by one quantity, the emission angle, and on this basis we may expect to be able to obtain the distributions $f_a(x, k_t^2, \mu^2)$ from single-scale evolution equations. Therefore it should be possible to follow an analytic approach where the physical assumptions are much more evident and where, in principle, NLO corrections can be included. Moreover, in practice, it is much easier to use the same unintegrated distributions to describe different hard processes and to perform global parton analyses.

The outline of this paper is as follows. The key observation is that the μ dependence of the unintegrated distributions enters at the last step of the evolution, and so we may use single-scale evolution equations. The procedure is first described in Section 2 in the case of pure DGLAP evolution, and then extended to include $\ln(1/x)$ effects in Section 3. In the latter case we use the solution of a single-scale equation which unifies DGLAP and BFKL evolution [4], and perform a final evolution step which brings in the dependence on the second scale. Ref. [5] also generated the two-scale unintegrated gluon from the same unified evolution equation, but

---

[1] This property is hidden in the conventional distributions as k_t is integrated up to the scale μ.

[2] At LO we have strong ordering of the emission angles, $\ldots \theta_i \ll \theta_{i+1} \ldots$; on the other hand if, at one step of the evolution $\theta_i \sim \theta_{i+1}$, then this contribution is included inside the NLO splitting function.

[3] The t-channel parton may have k_t up to μ/z, characteristic of BFKL effects, whereas for LO DGLAP the s and t-channel partons are both limited by $k_t < \mu$. Of course, some $k_t > \mu$ contribution will arise from the NLO splitting functions.

with a different procedure[4]. The unintegrated gluons obtained using the procedures described in Sections 2, 3 and Ref. [5] are compared in Section 4. In Section 5 we describe how the structure function F_2 is calculated from the unintegrated parton distributions, and in Section 6 we discuss the relationship between the unintegrated and integrated distributions. Finally in Section 7 we give our conclusions.

2 Unintegrated DGLAP partons

It is informative to review how unintegrated distributions $f_a(x, k_t^2, \mu^2)$ may be calculated from the conventional (integrated) parton densities, $a(x, \mu^2)$, in the case of pure DGLAP evolution. The procedure was explained in Ref. [6]. We start from the DGLAP equation[5]

$$\frac{\partial a(x, \mu^2)}{\partial \ln \mu^2} = \frac{\alpha_S}{2\pi} \left[\int_x^{1-\Delta} P_{aa'}(z) \, a'\left(\frac{x}{z}, \mu^2\right) dz - a(x, \mu^2) \sum_{a'} \int_0^{1-\Delta} P_{a'a}(z') dz' \right] \qquad (1)$$

where in the first term a sum over all possible parent partons a' is implied. This first term on the right-hand-side describes the number of partons δa emitted in the interval $\mu^2 < k_t^2 < \mu^2 + \delta\mu^2$. Such emission clearly changes the transverse momentum k_t of the evolving parton. If we were to neglect the virtual contribution in (1), then the unintegrated parton density would be given simply by

$$
\begin{aligned}
f_a(x, k_t^2) &= \left. \frac{\partial a(x, \mu^2)}{\partial \ln \mu^2} \right|_{\mu^2 = k_t^2} \\
&= \frac{\alpha_S(k_t^2)}{2\pi} \int_x^{1-\Delta} P_{aa'}(z) \, a'\left(\frac{x}{z}, k_t^2\right) dz.
\end{aligned}
\qquad (2)
$$

The virtual contribution in (1) does not change the parton k_t and may be resummed to give the survival probability T_a that parton a with transverse momentum k_t remains untouched in the evolution up to the factorization scale. The survival probability is given by

$$T_a(k_t, \mu) = \exp\left(-\int_{k_t^2}^{\mu^2} \frac{\alpha_S(k_t'^2)}{2\pi} \frac{dk_t'^2}{k_t'^2} \sum_{a'} \int_0^{1-\Delta} P_{a'a}(z') \, dz'\right), \qquad (3)$$

à la Sudakov form factor. Thus the probability to find parton a with transverse momentum k_t (which initiates a hard subprocess with factorization scale μ) is

$$f_a(x, k_t^2, \mu^2) = T_a(k_t, \mu) \left[\frac{\alpha_S(k_t^2)}{2\pi} \int_x^{1-\Delta} P_{aa'}(z) \, a'\left(\frac{x}{z}, k_t^2\right) dz \right]. \qquad (4)$$

---

[4]In this work we impose the angular ordering constraint in both the BFKL and DGLAP terms, and as a result do not have an exact equality between the integral up to μ^2 of the unintegrated distributions and the value of the integrated distribution. Ref. [5] takes the opposite approach; that is, exact equality with the integrated distribution is imposed and as a result angular ordering of the BFKL contribution is not complete. The difference is a NLO effect.

[5]For the $g \to gg$ splitting we have to insert a factor z' in front of $P_{gg}(z')$ in the last integral of (1) to account for the identity of the produced gluons.

It is at this *last step of the evolution* that the unintegrated distribution becomes dependent on the two scales, k_t^2 and μ^2.

We now have to take care to specify the value of the infrared cut-off Δ, which is introduced to protect the $1/(1-z)$ singularity in the splitting functions arising from soft gluon emission. In the original DGLAP equation, (1), which describes the evolution of the integrated distributions, this singularity is cancelled between the real emission and virtual contributions. However after the resummation of the virtual terms, the real soft gluon emission must be accounted for explicitly since it changes the k_t of the parton. Thus we have to find the physically appropriate choice of the cut-off Δ to provide the angular ordering of the gluon emissions[6].

In Ref. [6] the cut-off was taken to be $\Delta = k_t/\mu$. As a consequence the two-scale unintegrated distributions $f_a(x, k_t^2, \mu^2)$ of [6] vanish for $k_t > \mu$, in accordance with the DGLAP strong ordering in k_t. However we can do better and impose the more correct angular ordering in the last step of the evolution. It was shown in Refs. [1, 5] that this leads to a constraint on the scale μ, namely

$$\Theta(\theta - \theta') \;\; \Rightarrow \;\; \mu \; > \; z k_t/(1-z). \tag{5}$$

Thus the maximum allowed value of the integration variable z is

$$z_{max} \;\; = \;\; \frac{\mu}{\mu + k_t} \tag{6}$$

and the corresponding cut-off $\Delta = k_t/(\mu + k_t)$. Of course the same Δ must be used both in the real emission integral in (4) and in the survival probability T in (3).[7] In fact we shall see that the imposition of angular ordering at the last step of the evolution leads to physically reasonable parton k_t distributions which extend smoothly into the domain $k_t > \mu$.

3 Inclusion of $\ln(1/x)$ effects

We wish to generalize the above method to include the leading $\ln(1/x)$ contributions. Clearly there can be different forms of the 'unified' evolution equation summing up the leading DGLAP and BFKL logarithms, where the ambiguity is at the subleading level. The aim is to find a good prescription which is not too complicated, but which can account for all the physically relevant kinematic effects just at LO level. In other words we seek an equation which sums up the major part of the subleading corrections in a LO framework.

Let us consider, for the moment, just the gluon distribution. Recall that the unintegrated distribution $f(x, k_t^2, \mu^2)$ depends on two scales. As in the pure DGLAP case of Section 2 we wish to work in terms of a single-scale evolution equation, and then to restore the scale μ, and the full kinematics, at the last step of the evolution. This is illustrated schematically in Figure 1.

---

[6]Although the splitting functions P_{gq} and P_{qg} are not singular at $z = 1$ it is natural to use the same prescription for both the quark and the gluon distributions.

[7]In equation (3), $\Delta = k_t'/(\mu + k_t')$ is the appropriate cut-off for z'.

$f_a(x, k_t^2, \mu^2)$

$h_{a'}(x', k_t'^2)$
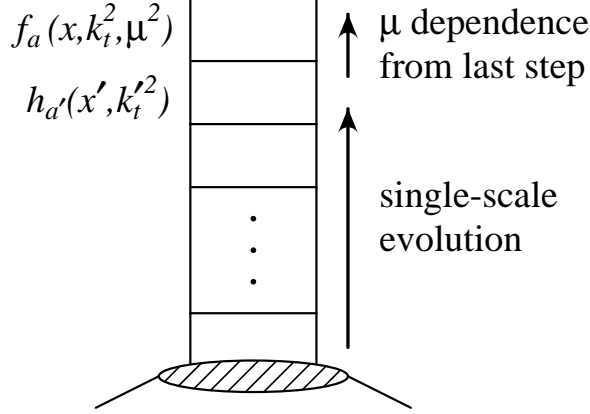
µ dependence from last step

single-scale evolution

Figure 1: An illustration of our procedure, in which the evolution of a single-scale unintegrated parton is followed by a final step of the ladder which introduces dependence on the second hard scale, μ.

For an analysis which incorporates BFKL effects, the appropriate single-scale distribution is the auxiliary function

$$h(x, k_t^2) = \frac{\partial(xg(x, k_t^2))}{\partial \ln k_t^2}. \tag{7}$$

Note that $h(x, k_t^2)$ is precisely the function which satisfies the BFKL equation in the low x limit.

Both BFKL and DGLAP evolution correspond to angular ordering of the emission angles, and are single-scale equations. At LO, strong angular ordering automatically comes either from strong ordering in x ($z \ll 1$) for BFKL or from strong k_t ordering ($k_t'^2 \ll k_t^2$) for DGLAP. For the unintegrated gluon, we face a problem when $k_t \sim \mu$ in the DGLAP framework, and similarly we have a problem when $z \sim 1$ for BFKL. Following the procedure of Ref. [6], we first neglect the subleading $k_t \sim \mu$ and $z \sim 1$ effects to obtain and solve a unified BFKL/DGLAP equation for $h(x, k_t^2)$. Then, in the last step of the evolution, we take account of the precise kinematics so that the $k_t \sim \mu$ and $z \sim 1$ domains are treated correctly.

The unified equation for h_g, which closely follows that presented in Ref. [4], takes the form

$$
\begin{aligned}
h_g(x, \mu^2) &= h_g^0(x, \mu^2) + \frac{\alpha_S(\mu^2)}{2\pi} \int_0^1 dz \int_{k_0^2}^{\mu^2} \frac{dk_t'^2}{k_t'^2} \left[\Theta(z - x)\, \bar{P}(z)\, h_g\left(\frac{x}{z}, k_t'^2\right) \right. \\
&\quad - z P_{gg}(z)\, h_g(x, k_t'^2) + \Theta(z - x) P_{gq}(z) \sum h_q\left(\frac{x}{z}, k_t'^2\right) - P_{gq}(z) \sum h_q(x, k_t'^2) \Big] \\
&\quad + \frac{\alpha_S(\mu^2)}{2\pi}\, 2N_C \int_x^1 \frac{dz}{z} \int_{k_0^2} \frac{dq^2}{q^2}\, \Theta(k_t'^2 - k_0^2) \left[\Theta(\mu^2 - zq^2) \frac{\mu^2}{k_t'^2}\, h_g\left(\frac{x}{z}, k_t'^2\right) \right. \\
&\quad - \Theta(\mu^2 - q^2)\, h_g\left(\frac{x}{z}, \mu^2\right) \Big],
\end{aligned}
\tag{8}
$$

where $\boldsymbol{k}_t' = \boldsymbol{k}_t + (1 - z)\boldsymbol{q}$, see Fig. 2.
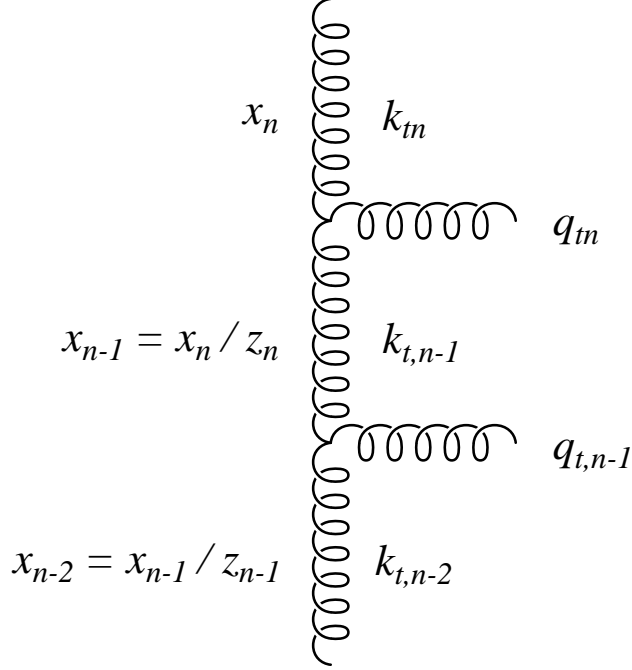
5

Figure 2: part of the evolution chain. We commonly write k_t for k_{tn} and then the parent's transverse momentum as k_t'. The radiated transverse momentum is q_t. Unified evolution is naturally performed [5] in terms of the rescaled transverse momentum $q_n = q_{tn}/(1 - z_n)$.

We have introduced single-scale unintegrated quark auxiliary functions $h_q(x, \mu^2)$ on the same footing as h_g,

$$h_q(x, \mu^2) = \frac{\partial(xq(x, \mu^2))}{\partial \ln \mu^2}, \tag{9}$$

and in (8) we sum over all $2n_F$ active flavours q of quarks and antiquarks with $m_q < \mu$. The h_q distributions satisfy the equation

$$h_q(x, \mu^2) = h_q^0(x, \mu^2) + \frac{\alpha_S(\mu^2)}{2\pi} \int_0^1 dz \int_{k_0^2}^{\mu^2} \frac{dk_t'^2}{k_t'^2} \left\{ \Theta(z - x) \left[P_{qg}(z) \, h_g\left(\frac{x}{z}, k_t'^2\right) \right.\right.$$

$$\left.\left. + \; P_{qq}(z) \, h_q\left(\frac{x}{z}, k_t'^2\right) \right] - P_{qq}(z) \, h_q(x, k_t'^2) \right\}, \tag{10}$$

which is the usual DGLAP equation for quark evolution written in terms of h_q of (9). The last term of (8) is the BFKL contribution which sums up all the leading $(\alpha_S \ln 1/x)^n$ terms, while the remaining terms on the right-hand-side describe the conventional DGLAP evolution of the gluon distribution with respect to scale μ^2. To avoid double counting, we have excluded the singular part of the P_{gg} splitting function in the real emission DGLAP term and used

$$\bar{P}(z) = P_{gg}(z) - \frac{2N_C}{z}. \tag{11}$$

The $2N_C/z$ term is already included in the BFKL contribution to (8).

6

The driving terms, h^0, which describe the low $k_t^2 < k_0^2$ domain are given by [4]

$$h_g^0(x, \mu^2) = \frac{\alpha_S(\mu^2)}{2\pi} \int_0^1 dz \left\{ \Theta(z - x) \left[P_{gg}(z) \frac{x}{z} g\left(\frac{x}{z}, k_0^2\right) \right. \right.$$

$$\left. \left. + P_{gq}(z) \sum \frac{x}{z} q\left(\frac{x}{z}, k_0^2\right) \right] - z P_{gg}(z) xg(x, k_0^2) - P_{gq}(z) \sum xq(x, k_0^2) \right\},$$

(12)

and similarly for h_q^0. The integrated input distributions $a(x, k_0^2)$ are not known and, as usual, must be determined from the data or from some non-perturbative QCD model.

We emphasize that in the unified BFKL/DGLAP equation we choose the scale μ to be k_t for the DGLAP contribution, to be consistent with the BFKL term (which is independent of μ at LO). Recall that angular ordering leads to a redefinition of the scale [1, 5]

$$\Theta(\theta - \theta') \implies \mu > zk_t/(1 - z).$$

If this modified scale were to be adopted then it would be impossible to obtain a simple one-scale unified evolution equation throughout the whole x, k_t^2 domain. On the other hand, within the LO framework, we may omit the z dependence in the scale, so that the DGLAP part of the evolution becomes ordered in transverse momenta. We stress again that it is sufficient to implement the precise constraints coming from angular ordering (relevant to the $z \sim 0$ and 1 domains for the BFKL and DGLAP terms respectively) at the last step of the evolution.

An advantage of the single-scale unified BFKL/DGLAP equation is that it is straightforward to incorporate a major (kinematical) part of the subleading order $\ln(1/x)$ (BFKL) effects[8] by imposing a consistency condition to ensure that the virtuality of the exchanged gluon is dominated by its transverse momentum squared [7]. This is achieved by the inclusion of the theta function $\Theta(\mu^2 - zq^2)$ in the real emission contribution shown in the last term of (8). Note that other subleading effects arising from using the complete DGLAP splitting function and running α_S are automatically included in the unified equation.

We see that the evolution equations for the auxiliary distributions $h_a(x, k_t^2)$ depend on the single scale k_t^2. The dependence of the unintegrated distributions $f_a(x, k_t^2, \mu^2)$ on the second scale μ will enter when we consider the *last step of the evolution*. It is sufficient to ensure that the final emitted parton explicitly satisfies the requirements of angular ordering. The angular ordering conditions of the previous steps of the evolution are automatically ensured at LO by virtue of either the strong ordering in k_t (in the DGLAP part) or the strong ordering in z (in the BFKL part).

To ensure angular ordering in the last step of the evolution, we note that z is limited by (5). This condition implies $z < \mu/(\mu + k_t)$, and so we take this as the upper limit of the z

---

[8]The large NLO BFKL corrections, which have recently been computed [8], appeared to have put the application of the BFKL framework into question. However a major part of the corrections is kinematic in origin and, when summed to all orders [7] using the theta function $\Theta(\mu^2 - zq^2)$, brings the BFKL approach back under control, see also [9, 10].

integration in (13) and (14) below. Thus the number of gluons produced at the last step (with transverse momentum k_t which initiate a hard subprocess with factorization scale μ) is[9]

$$
\begin{aligned}
f_g(x, k_t^2, \mu^2) \;=\;& T_g(k_t, \mu) \, \frac{\alpha_S(k_t^2)}{2\pi} \left\{ \int_x^{\mu/(\mu+k_t)} dz \int^{k_t^2} \frac{dk_t'^2}{k_t'^2} \left[\bar{P}(z) \, h_g\left(\frac{x}{z}, k_t'^2 \right) \right. \right. \\
&+ \left. P_{gq}(z) \sum h_q\left(\frac{x}{z}, k_t'^2 \right) \right] + 2N_C \int_x^{\mu/(\mu+k_t)} \frac{dz}{z} \int \frac{d^2q}{\pi q^2} \\
&\left. \left[\frac{k_t^2}{k_t'^2} \, h_g\left(\frac{x}{z}, k_t'^2 \right) \;-\; \Theta(k_t^2 - q^2) \, h_g\left(\frac{x}{z}, k_t^2 \right) \right] \right\},
\end{aligned}
\tag{13}
$$

and the number of a particular quark species q, produced at the last step, is

$$
\begin{aligned}
f_q(x, k_t^2, \mu^2) \;=\;& T_q(k_t, \mu) \, \frac{\alpha_S(k_t^2)}{2\pi} \int_x^{\mu/(\mu+k_t)} dz \int^{k_t^2} \frac{dk_t'^2}{k_t'^2} \left[P_{qg}(z) \, h_g\left(\frac{x}{z}, k_t'^2 \right) \right. \\
&+ \left. P_{qq}(z) \, h_q\left(\frac{x}{z}, k_t'^2 \right) \right].
\end{aligned}
\tag{14}
$$

This last step of the evolution is shown schematically in Fig. 1. The unintegrated distributions $f_a(x, k_t^2, \mu^2)$ represent the number of partons δa emitted in the $\delta \ln k_t^2$ interval from k_t^2 to $k_t^2 + \delta k_t^2$, and include the factors $T_a(k_t, \mu)$ of (3), which give the probabilities that partons $a = g, q$ with transverse momentum k_t remain untouched in the DGLAP evolution up to the factorization (probe) scale μ. These survival probabilities T_g and T_q resum the virtual DGLAP contributions occurring in (8) and (10) respectively.

It is important to note that the function $h_g(x, k_t^2)$ already includes the leading $\ln(1/x)$ virtual corrections, which have the effect of reggeizing the exchanged gluon; thus k_t is the total momentum transferred via the Regge gluon trajectory. Moreover, the distributions $f_a(x, k_t^2, \mu^2)$, evolved in the final step from the auxiliary functions $h_a(x, k_t^2)$, also incorporate the virtual DGLAP contributions, via the survival probabilities $T_a(k_t, \mu)$. The final expressions, (13) and (14), are thus more symmetric in that all the LO virtual corrections are included. That is, from a Feynman diagram viewpoint, the function $f_a(x, k_t^2, \mu^2)$ corresponds to the propagator of a t-channel parton of transverse momentum k_t, initiating a hard subprocess at scale μ, in which all the LO virtual corrections to the parton distribution have been taken into account.

4   The unintegrated gluon distribution

We have described how to obtain the (two-scale) unintegrated parton distributions $f(x, k_t^2, \mu^2)$ from the solution $h(x, k_t^2)$ of a one-scale equation which unifies DGLAP and BFKL evolution. The link is (13), (14), which represent the last step of the evolution. Only at this stage does the scale μ of the subprocess, initiated by $f(x, k_t^2, \mu^2)$, enter.

---

[9]The low $k_t < k_0$ domain of the integrals in (13), (14) should be treated as the driving terms h^0 in (12).

It is informative to compare the unintegrated gluon distribution $f_g(x, k_t^2, \mu^2)$ with the behaviour of the auxiliary function $h_g(x, k_t^2)$. Consider first the pure BFKL limit, in which DGLAP evolution is neglected, that is $\alpha_S \ln \mu^2 \ll 1$, but $\alpha_S \ln 1/x \gtrsim 1$. Then, in (13), the survival probability $T_g(k_t, \mu) = 1$ and there are no DGLAP contributions. Thus we obtain

$$f_g(x, k_t^2, \mu^2) \;=\; h_g(x, k_t^2) \;=\; \frac{\partial(xg(x, k_t^2))}{\partial \ln k_t^2}. \tag{15}$$

This is an expression which is frequently used at low x.

When x is sufficiently large, the derivative

$$h_a \;=\; \frac{\partial(a(x, k_t^2))}{\partial \ln k_t^2} \tag{16}$$

becomes negative, even for $k_t \lesssim \mu$. The reason is that the negative virtual DGLAP term exceeds the real emission DGLAP contribution, which is suppressed by the large lower limit $z > x$ in (8), (10), (13) and (14). After the virtual contributions are resummed into the T_a factors the unintegrated parton distributions remain positive everywhere.

We already stated in Section 2 that imposing angular ordering on the last step of "DGLAP" evolution caused the distribution to extend smoothly into the $k_t > \mu$ domain. The gluons also populate this domain due to BFKL diffusion in $\ln k_t^2$. This raises the question of how much enhancement we find in this domain due to the inclusion of the BFKL contributions. To investigate this point, we compute the unintegrated gluon distribution $f_g(x, k_t^2, \mu^2)$ in two different ways.

(a) In the first approach, the function $h_g(x, k^2)$ of Ref. [4] is used as the auxiliary function to drive the last-step evolution in (13) and (14). This incorporates essentially maximal BFKL effects.[10]

(b) In the second case, we use unintegrated "DGLAP" partons to drive the two-scale unintegrated f_a via (4). This approach is essentially pure DGLAP, but with the crucial modification that the cut-off in (3) and (4) is motivated by *angular ordering*. Here we use the MRST99 [11] set of partons as input.

Ideally, we should refit to the deep inelastic and related scattering data and perform global *unintegrated* parton analyses[11] in terms of $f_a(x, k_t^2, \mu^2)$, since now we have added an extra last step to the evolution. However, such global analyses are beyond the scope of the present paper.

The unintegrated gluon distribution $f_g(x, k_t^2, \mu^2)$, obtained by the two alternative procedures (a) and (b), is shown in Fig. 3 for $\mu = 10$ GeV. We can compare the continuous curves

---

[10]In comparison with (10), the evolution of h_q in Ref. [4] contains some resummation of the BFKL-like leading $(\alpha_S \ln 1/x)^n$ terms.

[11]In Section 5, we describe the theoretical calculation of F_2, the most important observable for constraining parton sets, from the two-scale unintegrated f_g and f_q.

of approach (a) directly with the previous unintegrated gluon distribution (dashed curves) calculated in Ref. [5], which also used the same auxiliary function $h_g(x, k_t^2)$ of [4] as input. For $k_t < \mu$ the new results tend to lie above the previous determination [5], while for $k_t > \mu$ they are increasingly smaller as k_t increases. In the present work, the decrease at large k_t arises from the restriction $z < z_{\max} = \mu/(\mu + k_t)$, whereas the earlier calculation, based on eq. (23) of Ref. [5], omitted the limit $z < z_{\max}$ on the BFKL contribution, which causes f_g to increase in the large k_t domain at small values of x.

Finally we compare the DGLAP-like unintegrated gluon, obtained in approach (b), with that of approach (a) which embodied BFKL evolution. That is we compare the dotted with the continuous curves of Fig. 3. It is interesting to note that, with the more precise angular-ordered (CCFM [1]) cut-off from (5), $\Delta = k_t/(\mu + k_t)$, the unintegrated gluon distribution (b) generated from (4) using the pure DGLAP MRST99 [11] partons turns out to be very similar to the result (a) obtained using the auxiliary function h_g. This coincidence can be explained by the facts (i) that both the DGLAP partons and the analysis of Ref. [4] (which yielded h_g) fit the deep inelastic data well, and (ii) that both these input are used with the same angular-ordered constraint, (5). We draw the conclusion that the role of angular ordering in the last step of evolution is particularly important, even more so than BFKL effects in the HERA domain.

5 F_2 calculated from the unintegrated partons

To check the reliability of our unintegrated parton distributions, and to demonstrate how to use these distributions in calculations of observables, we compute the deep inelastic structure function F_2. We wish to treat the unintegrated gluons and unintegrated quarks on an equal footing as input to the subprocess cross sections, so we explicitly separate gluon and (direct) quark contributions to F_2.

The gluon contributes to F_2 via the quark box and crossed-box diagrams of Fig. 4. These generate, via the $g \to q\bar{q}$ splitting, a sea quark contribution S_q to F_2 of the form [12, 4]

$$F_2^{g \to q\bar{q}}(x, Q^2) \;=\; \sum_q e_q^2 \, S_q(x, Q^2), \tag{17}$$

with

$$S_q(x, Q^2) \;=\; \frac{Q^2}{4\pi^2} \int \frac{dk_t^2}{k_t^4} \int_0^1 d\beta \int d^2\kappa_t \, \alpha_S(\mu^2) \, f_g\left(\frac{x}{z}, k_t^2, \mu^2\right) \, \Theta\left(1 - \frac{x}{z}\right)$$

$$\left\{ \left[\beta^2 + (1-\beta)^2\right] \left(\frac{\boldsymbol{\kappa}_t}{D_1} - \frac{\boldsymbol{\kappa}_t - \boldsymbol{k}_t}{D_2}\right)^2 + \left[m_q^2 + 4Q^2\beta^2(1-\beta)^2\right] \left(\frac{1}{D_1} - \frac{1}{D_2}\right)^2 \right\}. \tag{18}$$

The denominator factors are

$$D_1 \;=\; \kappa_t^2 \;+\; \beta(1-\beta)\, Q^2 \;+\; m_q^2$$

$$D_2 \;=\; (\boldsymbol{\kappa}_t - \boldsymbol{k}_t)^2 \;+\; \beta(1-\beta)\, Q^2 \;+\; m_q^2. \tag{19}$$
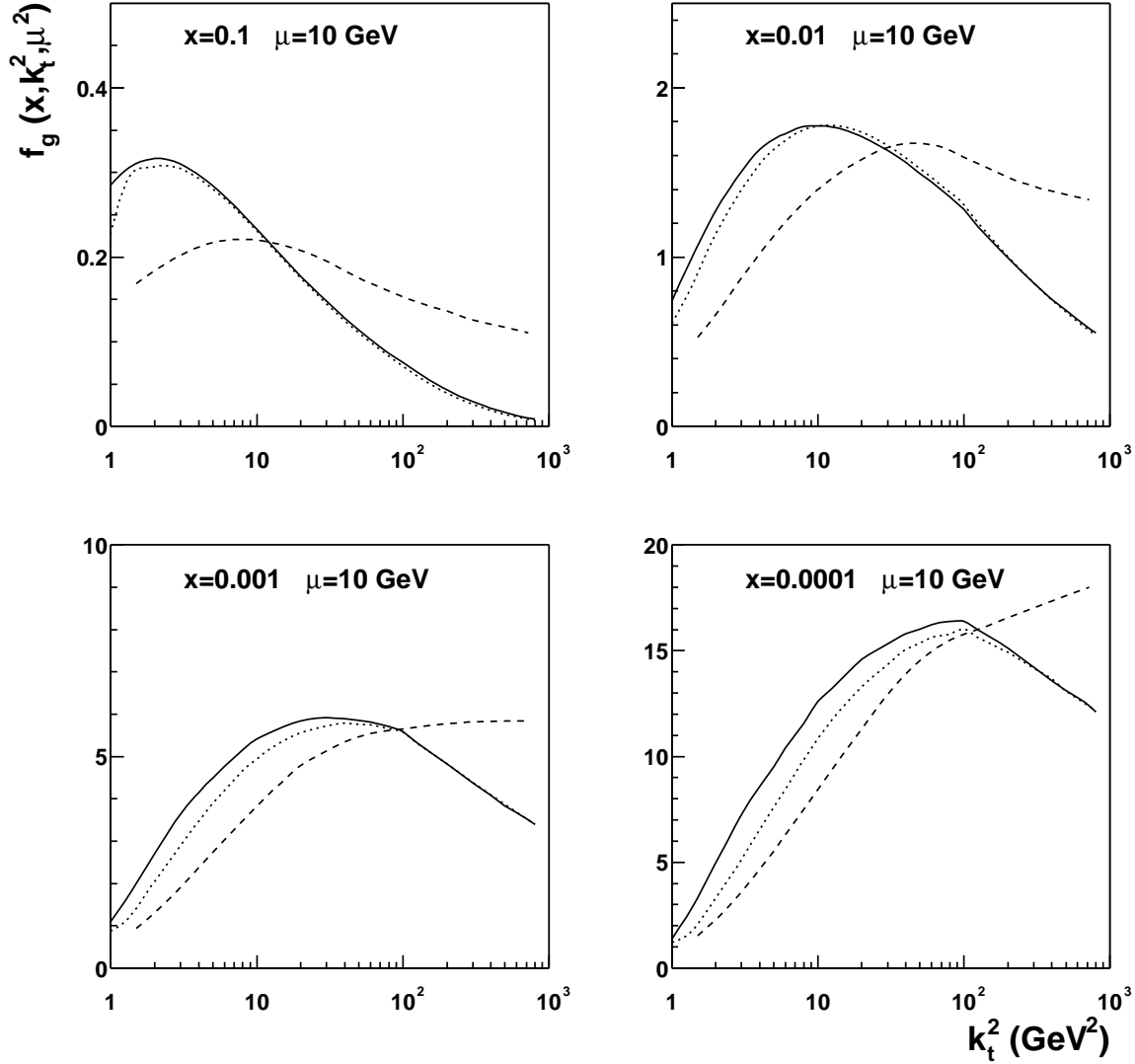
10

Figure 3: plots of the k_t-dependence of the unintegrated gluon $f_g(x, k_t^2, \mu^2)$ for various values of x, at $\mu = 10$ GeV. The solid curves are our version (a) of f_g from (13); for comparison we show with dashed lines the unintegrated gluon from [5] (as in [5], the dashed lines have been smoothed in the transition region $k_t \sim \mu$). Also we plot our "DGLAP" unintegrated gluon (b) from (4) in dotted lines, which with the correct angular ordering cut-off is very close to the new f_g, especially at high x.
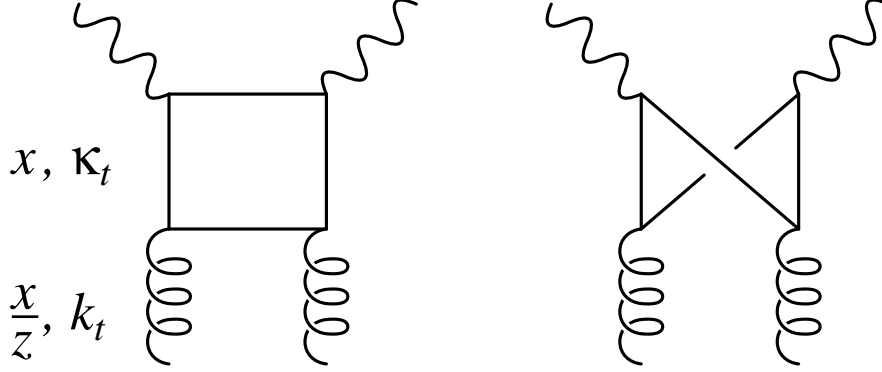
11

Figure 4: The quark box, and crossed-box, diagrams which mediate the contribution of the unintegrated gluon distribution $f_g(x/z, k_t^2, \mu^2)$ to F_2.

We may exploit the symmetry of the integrand in (18) under $\boldsymbol{\kappa}_t \to \boldsymbol{\kappa}_t - \boldsymbol{k}_t$ and $\beta \to 1 - \beta$ to rewrite $\{\ldots\}$ as

$$
2\left\{\left[\beta^2 + (1-\beta)^2\right]\left(\frac{\kappa_t^2}{D_1^2} - \frac{\kappa_t^2 - \boldsymbol{\kappa}_t \cdot \boldsymbol{k}_t}{D_1 D_2}\right) + \left[m_q^2 + 4Q^2\beta^2(1-\beta)^2\right]\left(\frac{1}{D_1^2} - \frac{1}{D_1 D_2}\right)\right\}.
\tag{20}
$$

The summation in (17) is over massless u, d, s quarks and a c quark of mass $m_c = 1.4$ GeV; there is no need to sum $\bar{u}$, $\bar{d}$, $\bar{s}$, $\bar{c}$ in addition, because as (18) is written, S_u, say, is the contribution of a gluon via a u quark box of any momentum. The variable β is the light-cone fraction of the photon momentum carried by the internal quark. The variable z is the ratio of Bjorken x and the fraction of the proton momentum carried by the gluon. It is specified by the relation

$$
\begin{aligned}
\frac{1}{z} &= 1 + \frac{(\boldsymbol{\kappa}_t - (1-\beta)\boldsymbol{k}_t)^2 + m_q^2}{\beta(1-\beta)Q^2} + \frac{k_t^2}{Q^2} \\[2mm]
&= 1 + \frac{\kappa_t^2 + m_q^2}{(1-\beta)Q^2} + \frac{k_t^2 + \kappa_t^2 - 2\boldsymbol{\kappa}_t \cdot \boldsymbol{k}_t + m_q^2}{\beta Q^2},
\end{aligned}
\tag{21}
$$

which is obtained by requiring the outgoing quarks to be on-shell. Following Ref. [4], we choose the scale μ which controls the unintegrated gluon distribution and the QCD coupling α_S to be

$$
\mu^2 = k_t^2 + \kappa_t^2 + m_q^2.
\tag{22}
$$

Care is needed in separating this calculation into perturbative and non-perturbative regions. We impose a cut-off $k_t > k_0$ for a legitimate perturbative calculation of (18). The smallest cut-off we can choose is the minimum (that is, initial) scale of the function $h_g(x, k_t^2)$ from which our two-scale distributions derive. Thus k_0 is of order 1 GeV. For the contribution from the

region of $k_t < k_0$ we approximate

$$\int_0^{k_0^2} \frac{dk_t^2}{k_t^2} f_g(x, k_t^2, \mu^2) \left[\frac{\text{remainder}}{k_t^2} \right] \simeq xg(x, k_0^2) T_g(k_0, \mu) \left[\quad \right]_{k_t=a}, \qquad (23)$$

where a can be taken to be any value representative of the interval $(0, k_0)$. The dependence on the choice of a is numerically unimportant.

Now we have to add the direct quark contributions to F_2, which come from the unintegrated quark distributions $f_q(x, k_t^2, \mu^2)$. If a quark, initially with x/z and perturbative transverse momentum $k_t' > k_0$, splits to a radiated gluon and a 'final'[12] quark with Bjorken x and transverse momentum κ_t, then this final quark can couple to the photon and contribute to F_2 as:

$$F_2^{q(\text{pert})}(x, Q^2) = \sum_q e_q^2 \int_{k_0^2}^{Q^2} \frac{d\kappa_t^2}{\kappa_t^2} \frac{\alpha_S(\kappa_t^2)}{2\pi} \int_{k_0^2}^{\kappa_t^2} \frac{dk_t^2}{k_t^2} \int_x^{Q/(Q+k_t)} dz$$

$$\left[f_q\left(\frac{x}{z}, k_t^2, Q^2\right) + f_{\bar{q}}\left(\frac{x}{z}, k_t^2, Q^2\right) \right] P_{qq}(z). \quad (24)$$

where here we have written the antiquark contribution explicitly. As in (14), the upper limit of the z integration reflects the angular-ordered constraint of (5) during the quark evolution.

Again we need to account for the non-perturbative domain $k_t < k_0$. The initial (integrated) quark distribution $xq(x, k_0^2)$ drives our final contribution. Physically the only remaining diagrams that we have not included are those in which a quark (or antiquark) from this initial distribution does not experience real splitting in the perturbative domain, but interacts unchanged with the photon at scale Q. Hence we write a Sudakov-like factor $T_q(k_0, Q)$ to represent the probability of evolution from k_0 to Q without radiation.

$$F_2^{q(\text{non-pert})}(x, Q^2) = \sum_q e_q^2 \left(xq(x, k_0^2) + x\bar{q}(x, k_0^2) \right) T_q(k_0, Q). \qquad (25)$$

To avoid double counting, it is important to put a lower limit on κ_t in both (18) and (24), by enforcing $\Theta(\kappa_t^2 - k_0^2)$ in the integrations. Without this lower limit on the final transverse momentum κ_t, equations (18) and (24) would partially include low transverse momentum κ_t quark contributions which are best incorporated in (25), whether they originate from partons with $k_t > k_0$ or not.

The structure function $F_2(x, Q^2)$ is given by the sum of the gluon-initiated contribution (17), and the quark terms, (24) and (25). In Fig. 5 sample results[13], shown by the continuous curves, are compared with deep-inelastic structure function data. The gluon and quark components are shown by the dashed and dotted curves respectively. As expected the dominant contribution at small x comes from the unintegrated gluon via the quark box and crossed-box contributions, whereas at large x the quark terms dominate.

---

[12]By 'final' we mean the struck quark just after the P_{qq} splitting.

[13]We show in Fig. 5 results obtained using the unintegrated distributions evaluated from (4) with the MRST99 partons [11], that is, version (b) of f_g and f_q as discussed in Section 4.

We emphasize that, in the present work, the curves for F_2 are not the result of a fit to the structure function data. Rather they have been obtained by using single-scale functions, originally fitted more directly to F_2 data, as plausible input to our 'last-step' evolution procedure, which generates two-scale unintegrated distributions $f_a(x, k_t^2, \mu^2)$. Then we use the unintegrated distributions to compute F_2 via (17), (24) and (25). For the inclusive observable F_2, we would expect that the insertion of this extra evolution step would not appreciably disturb the description, since it essentially redistributes the distributions in k_t space. We see from Fig. 5 that indeed this is the case.

6   Relation of f to integrated partons

It is important to scrutinise the relationship between the new unintegrated partons $f_a(x, k_t^2, \mu^2)$ and the conventional integrated parton distributions $a(x, \mu^2)$, as obtained in global analyses such as [11]. First we emphasize that we may use either the integrated distributions or the unintegrated distributions to describe both inclusive (like F_2) and exclusive processes. The framework based on the unintegrated distributions is a bit more complicated. However it accounts for the precise kinematics of the process and an important part of the virtual loop corrections, via the survival factor T, even at LO. On the other hand, if we work with integrated partons we have to include NLO (and sometimes NNLO) contributions to account for these effects. These differences appear to cause a discrepancy between the integrated and unintegrated approaches. As we explain below, this is to be expected since it arises from simplifications of the LO formalism due to the neglect of terms which are moved into the NLO contribution.

An important equation, sometimes cited as the defining property of unintegrated partons [5], is

$$a(x, \mu^2) = \int^{\mu^2} \frac{dk_t^2}{k_t^2} f_a\left(x, k_t^2, \mu^2\right), \tag{26}$$

where a represents xg or xq. This is in fact the first equation of Ref. [5]. In the BFKL limit, the μ dependence of f vanishes and we have $f_g(x, k_t^2, \mu^2) \to h_g(x, k_t^2)$ as in (15). In this case, (26) is clearly satisfied. However, in general the situation is complicated by the two separate momentum scales k_t and μ. The unintegrated partons f_g of Ref. [5] were explicitly constructed to have the property (26), in the sense that the integral of f_g over the transverse momentum up to the scale μ would be the same as the integral of the input auxiliary function $h_g(x, k_t^2)$ up to the same scale. In contrast, numerical integration over k_t of the new unintegrated partons f_g and f_q presented in this paper (both versions (a) and (b) of Section 4) shows that (26) is only approximately true.[14] We typically find a discrepancy of order 25% between the right-hand side of (26) and the single-scale distribution that has been used to generate f_a.

---

[14]Note that we cannot compute (26) as it is written, because we can only define the unintegrated function in the regime of perturbative $k_t > k_0$. The comparison that is made is between the integral from k_0^2 to μ^2 and the quantity $a(x, \mu^2) - a(x, k_0^2)$.
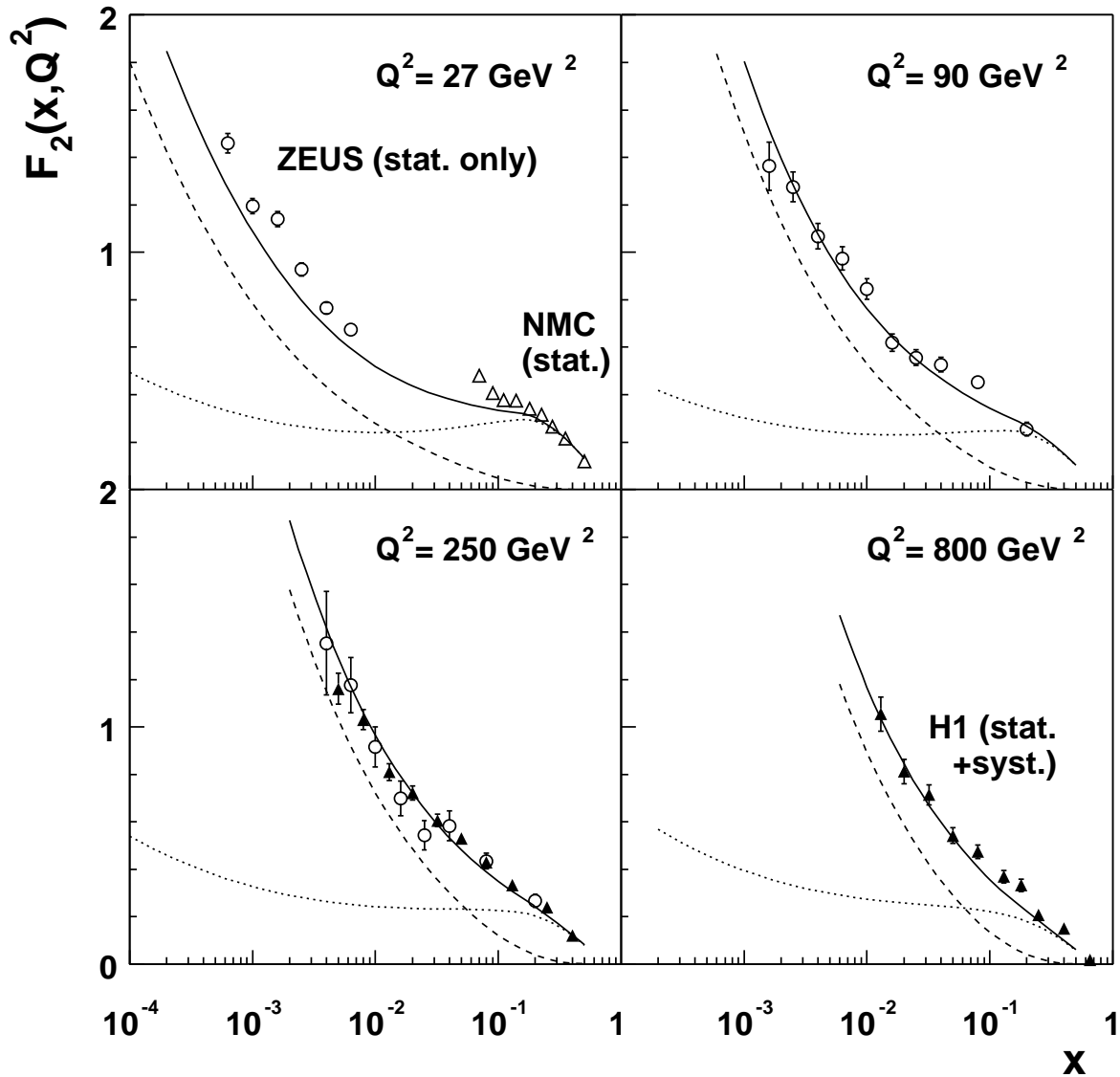
Figure 5: This is not a fit but the results of using our "DGLAP" unintegrated partons (b) to calculate F_2; the gluon-originated contributions are shown as dashed lines and the quark-originated parts are shown as dotted lines. Recent data are plotted [13], and compare well with the sum of the gluon and quark contributions (solid curves), especially at high Q^2.

In order to eliminate the discrepancy we may adjust the upper limit μ^2 of the integral in (26) to $c^2\mu^2$. The introduction of c is equivalent to a NLO correction for the integrated partons. Typically in the "DGLAP" case (approach (b) of Section 4) we require $c = 0.6 - 0.8$ to reproduce[15] the original MRST integrated gluon in the domain $\mu = 5 - 10$ GeV and $x \lesssim 0.01$ (and $c \approx 0.4$ for approach (a), which embodies BFKL effects). A value $c < 1$ compensates for the over-large virtual loop correction included in the integrated DGLAP partons on account of the absence of the cut-off Δ in the integral over z'. At smaller values of x the corrections due to the cut-off are mainly cancelled between the virtual and real DGLAP contributions. As x increases, the virtual contribution (the second term on the right-hand-side of (1)) increasingly dominates and we have to choose smaller values of c. Eventually in the domain $x > 0.1$, $\mu \sim 10$ GeV the main contribution comes from the input and to compensate the absence of the z cut-off in the conventional form of the DGLAP equation we must change the input itself.

To summarize, the discrepancy between the integral (26) of the unintegrated parton function and the original integrated distribution is not a cause for concern. Conceptually, there are two different roles for single-scale distributions in the description of data for inclusive observables (where partonic transverse momentum is integrated out). The first role is the traditional one, in the framework of collinear factorization, whereby integrated parton distribution functions are fitted directly to the data. The second role is demonstrated in this paper (following [6] and [5]), where we use single-scale functions as *input* to the last-step procedure, see for example (4). We have been forced to introduce a new formalism for calculating $F_2(x, Q^2)$, in which unintegrated parton functions are understood to be the fundamental objects; we have emphasized the need to perform a new global fit to data in terms of the new functions f_a. After this, we do not expect the input single-scale function a on the left-hand side of (26) to equal the integral of f_a up to μ^2, since a itself is not fitted directly to the data, but rather is used as input for the last step of the evolution, which embodies a crucial angular-ordering constraint unique to this last step. Thus our single-scale or 'auxiliary' function is not a traditional parton distribution function, but simply an intermediate function.

7 Conclusions

Parton distributions, $f_a(x, k_t^2, \mu^2)$ unintegrated over the parton k_t are the basic quantities for describing processes initiated by hadrons. An essential ingredient in this description is the existence of the k_t factorization theorem [14]. The unintegrated distributions depend on two hard scales — the transverse momentum k_t and the factorization scale μ. The scale μ drives the angular ordering during the evolution which arises from the coherence of the gluon emissions.

Here we develop a new formalism to determine the unintegrated parton distributions, $f_a(x, k_t^2, \mu^2)$, which embodies both the leading $\ln Q^2$ (DGLAP) and $\ln 1/x$ (BFKL) effects,

---

[15]This identification is only approximate since the last step of the evolution is not included in the comparison.

as well as including a major part of the sub-leading $\ln 1/x$ contributions. An important observation is that, at leading order, the *two-scale* functions $f_a(x, k_t^2, \mu^2)$ may be calculated from auxiliary functions $h_a(x, k_t^2)$ which satisfy *single-scale* evolution equations, since the angular ordering restrictions, controlled by μ, become important only at the last step of the evolution. The equation for the auxiliary function $h_g(x, k_t^2)$ was formulated, and the distributions fitted to the data, in Ref. [4]. These single-scale equations were also devised to include all the leading $\alpha_S \ln Q^2$ and $\alpha_S \ln 1/x$ contributions, and a major part of the sub-leading $\ln 1/x$ effects.

In other words, the 'unified' evolution equations for h must be supplemented by a final evolution step in which the μ dependence of the unintegrated parton distributions enters via the angular-ordering constraint. The situation is summarised diagrammatically in Fig. 1. The procedure offers a considerable simplification in the determination of physically realistic unintegrated parton distributions $f_a(x, k_t^2, \mu^2)$ over the full x, μ^2 perturbative domain, including the true kinematics even at leading order. As expected, the gluon and sea quark distributions extend into the $k_t > \mu$ region more and more as x decreases. We have compared the new unintegrated distributions with those given by previous prescriptions [6, 5]. As compared to Ref. [5], the new formalism gives a consistent treatment of angular ordering, which leads to the imposition of the z integration limit $z < \mu/(\mu + k_t)$. As a consequence the distributions $f_a(x, k_t^2, \mu^2)$ decrease faster than those of [5] for large k_t, particularly at small x. An interesting result is that the unintegrated distributions obtained via $h_a(x, k_t^2)$ of [4] are not very different from those obtained via (4) using conventional DGLAP partons — compare the continuous and dotted curves in Fig. 3. It thus appears that the imposition of the angular-ordering constraint is more important than the BFKL effects. This observation has the practical consequence that reasonably accurate predictions for observables can be made using the much simpler, though less complete, prescription of (4).

Finally, we used the new unintegrated distributions to calculate the deep-inelastic structure function F_2. We also showed the gluon-initiated and quark contributions separately, which, as expected, dominate at small x and large x respectively. Recall, from [4], that the rise of the gluon at small x is driven by perturbative QCD, which was assumed to have a non-perturbative input which is 'flat' in x. We emphasize that we have not fitted to the deep inelastic data. Nevertheless, Fig. 5 shows that the existing distributions give an adequate description, and therefore they may be used to evaluate other hard processes, such as $b\bar{b}$ and large q_t prompt photon production in high energy $p\bar{p}$ (or pp) collisions. It is important to use unintegrated distributions for such exclusive reactions.

Acknowledgements

References

[1] M. Ciafaloni, Nucl. Phys. **B296** (1988) 49;
S. Catani, F. Fiorani and G. Marchesini, Phys. Lett. **B234** (1990) 339; Nucl. Phys. **B336** (1990) 18;
G. Marchesini, in Proceedings of the Workshop "QCD at 200 TeV", Erice, Italy, 1990, edited by L. Cifarelli and Yu.L. Dokshitzer, (Plenum Press, New York, 1992), p.183.

[2] J. Kwiecinski, A.D. Martin and P.J. Sutton, Phys. Rev. **D52** (1995) 1445;
G. Bottazzi, G. Marchesini, G.P. Salam and M. Scorletti, Nucl. Phys. **B505** (1997) 366;
JHEP 9812 (1998) 011.

[3] G. Marchesini and B. Webber, Nucl. Phys. **B349** (1991) 617; **B386** (1992) 215;
H. Jung, Nucl. Phys. Proc. Suppl. **79** (1999) 429;
H. Jung and G.P. Salam, `hep-ph/0012143`;
H. Kharraziha and L. Lönnblad, JHEP 98003 (1998) 006.

[4] J. Kwiecinski, A.D. Martin and A.M. Stasto, Phys. Rev. **D56** (1997) 3991.

[5] M.A. Kimber, J. Kwiecinski, A.D. Martin and A.M. Stasto, Phys. Rev. **D62** (2000) 094006.

[6] M.A. Kimber, A.D. Martin and M.G. Ryskin, Eur. Phys. J. **C12** (2000) 655.

[7] J. Kwiecinski, A.D. Martin and P.J. Sutton, Z. Phys. **C71** (1996) 585.

[8] V.S. Fadin and L.N. Lipatov, Phys. Lett. **B429** (1998) 127;
M. Ciafaloni and G. Camici, Phys. Lett. **B430** (1998) 349.

[9] B. Andersson, G. Gustafson and J. Samuelson, Nucl. Phys. **B467** (1996) 443;
B. Andersson, G. Gustafson, H. Kharraziha and J. Samuelson, Z. Phys. **C71** (1996) 613.

[10] G.P. Salam, JHEP **07** (1998) 19;
M. Ciafaloni and D. Colferai, Phys. Lett. **B452** (1999) 372;
M. Ciafaloni, D. Colferai and G.P. Salam, Phys. Rev. **D60** (1999) 114036.

[11] A.D. Martin, R.G. Roberts, W.J. Stirling and R.S. Thorne, Eur. Phys. J. **C14** (2000) 133.

[12] A.J. Askew, J. Kwiecinski, A.D. Martin and P.J. Sutton, Phys. Rev. **D47** (1993) 3775.

[13] NMC: Arneodo et al., Nucl. Phys. **B483** (1997) 3;
ZEUS: Derrick et al., Zeit. Phys. **C72** (1996) 399;
H1: Adloff et al., Eur. Phys. J. **C13** (2000) 609.

[14] S. Catani, M. Ciafaloni and F. Hautmann, Phys. Lett. **B242** (1990) 97; Nucl. Phys. **B366** (1991) 135;
J.C. Collins and R.K. Ellis, Nucl. Phys. **B360** (1991) 3;
E.M. Levin, M.G. Ryskin, Yu.M. Shabelski and A.G. Shuvaev, Sov. J. Nucl. Phys. **54** (1991) 867.